Appl. Magn. Reson. 17, 557−576 (1999)

^{73}Ge NMR Spectra in Germanium Single Crystals with Different Isotopic Composition

S. V. Verkhovskii[1], A. Yu. Yakubovskii[2], A. Trokiner[3], B. Z. Malkin[4], S. K. Saikin[4], V. I. Ozhogin[2], A. V. Tikhomirov[2], A.V. Ananyev[1], A. P. Gerashenko[1], and Yu. V. Piskunov[1]

[1] Institute of Metal Physics, Russian Academy of Sciences, Ekaterinburg, Russian Federation
[2] Russian Research Center "Kurchatov Institute", Moscow, Russian Federation
[3] Ecole Superieure de Physique et de Chimie Industrielles, Paris, France
[4] Kazan State University, Kazan, Russian Federation

Received August 25, 1999

Abstract. We have studied the influence of isotopic disorder on the local deformations in Ge single crystals from both experimental and calculation points of view. The nuclear magnetic resonance (NMR) spectra of ^{73}Ge nuclei (the nuclear spin equals 9/2) in perfect single crystals of germanium with different isotopic content were measured at temperatures 80, 300 and 450 K. Abnormal broadening of the spectrum was found to occur when the magnetic field was aligned along the [111] axis of a crystal. The observed specific angular dependence of the quadrupole broadening was attributed to isotopic disorder among atoms of germanium sited around the ^{73}Ge NMR probe. Local lattice deformations in germanium crystal lattice due to isotopic impurity atoms were calculated in the framework of the adiabatic bond charge model. The results obtained were applied to study random noncubic crystal field interactions with the nuclear quadrupole moments and corresponding effects in NMR spectra. Simulated second and fourth moments of resonance frequency distributions caused by the magnetic dipole-dipole and electric quadrupole interactions are used to analyze the lineshapes, theoretical predictions agree qualitatively with the experimental data.

1 Introduction

In perfect crystals the electric field gradient (EFG) at atomic nuclei with cubic symmetry of the charge environment is zero. Magnetic energy levels of quadrupole nuclei ($I > 1/2$), characterized by spin projections m_I on the magnetic field, are spaced equidistantly. The single nuclear magnetic resonance (NMR) signal should be expected in this case with the width of the spectral line which is determined only by magnetic spin-spin interactions. Crystal lattice defects would destroy cubic symmetry of the charge distribution around an atom positioned near a defect. As a result, additional broadening of the NMR line would occur due to the nonvanishing quadrupolar shifts ($\Delta E_Q \sim m_I^2 V_{zz}$) of Zeeman energy levels. The change of the EFG (V_{zz}) around the lattice defect depends on its origin. The

influence of traditional defects in crystals (dislocations, vacancies and impurity atoms) on the shape and the intensity of NMR line are discussed in some excellent reviews [1, 2].

In this paper we would like to attract attention at another kind of structural disorder widely occurring in crystals. This is isotopic disorder among atoms of the same chemical element. The dynamic effect of isotopic disorder on the phonon scattering process, which manifests as one of the main contributions to thermal conductivity at low temperatures [3, 4], is well known. In static phenomena the isotopic disorder in real crystals causes a random distribution of the interionic distances and a corresponding random distribution of the crystal electric fields affecting the quadrupole moment of nuclei. The most pronounced effect of the isotopic disorder should be expected in cubic crystals. Single crystals of germanium represent the acme among them. Advanced technology of synthesis permits one to grow Ge single crystals having a minimal concentration of traditional defects mentioned above. A rather large quadrupole moment of the ^{73}Ge isotope ($I = 9/2$, $Q = -0.19$ barn) provides high sensitivity of the NMR experiments to detect small deviations from cubic symmetry around resonant nuclei. The further increase of experimental performance can be achieved in single crystals predominantly enriched by an isotope without nuclear paramagnetism, like ^{74}Ge. Magnetic spin-spin interactions in these crystals are reduced greatly, and NMR of the ^{73}Ge isotope as an impurity atom will represent extremely high sensitivity to detect small lattice deformations due to the isotopic disorder. In the framework of the harmonic approximation a change in isotopic composition results only in changes of the vibration spectrum of the crystal lattice. Distances between atoms, as in the thermal expansion, experience variations only as a consequence of the anharmonicity of vibrations. In the limit of high temperatures, the lattice constant is independent of atomic masses. Thus, studies of the random crystal field induced by the isotopic disorder provide information on the macroscopic quantum effect.

In Sect. 2, the specific peculiarities of the NMR signals of quadrupole nuclei due to the isotopic disorder in the cubic crystal lattice are studied. NMR line shape dependence on the isotopic composition and temperature is considered. In Sect. 3, ^{73}Ge NMR spectra measured in crystals with different isotopic content for different orientations of the magnetic field with respect to crystallographic axes as well as some experimental details are presented. We analyze experimental results in Sect. 4, the simulated spectral envelopes of the ^{73}Ge NMR line are compared with the measured spectra. Calculations of the local static lattice deformations induced by the impurity isotopes in the framework of the adiabatic bond charge model (ABCM) of Weber [5] are described in the appendix.

2 Quadrupole Line Broadening Induced by the Isotopic Disorder in the NMR Spectra

The isotopic disorder in real crystals causes random distribution of the interionic distances and the corresponding random distribution of the crystal electric fields

affecting the nuclear quadrupole moments. In the present work, ABCM is used to obtain both the lattice deformations, induced by the isotopic disorder, and the electric field gradient at the magnetic ^{73}Ge nuclei. This model has been successfully employed to describe the phonon spectrum of Ge [5] and anharmonic effects in the spectra of the Si/Ge heterostructures [6]. A bond charge $(-Z_b e)$ is placed on each bond connecting two adjacent Ge atoms. Each atom has four bonds of the $a\sqrt{3}/4$ length (a is the lattice constant), and the atomic charge is equal to $Z_a e = 2Z_b e$. In the ideal lattice a bond charge is frozen in the midway position between the corresponding atoms. In the vibrating lattice the massless bond charges move due to Coulomb and non-Coulomb forces which appear when atoms and bond charges displace from their equilibrium positions. In the general case, the magnitude of the bond charge depends on the bond length [6]. In this work, we consider the constant value of the bond charge $Z_b = 1.61$ which has been already used in lattice dynamics calculations [5] and approved in the analysis of the nuclear spin-lattice relaxation of ^{73}Ge induced by thermal fluctuations of EFG in a perfect Ge crystal without isotopic disorder [7].

The Hamiltonian of the ^{73}Ge nucleus subsystem in the strong applied magnetic field H ($H \gg \gamma\hbar/a^3$, where $\gamma\hbar I = -0.8795\mu_N$ is the ^{73}Ge magnetic moment) can be presented as

$$\mathscr{H} = \sum_j \mathscr{H}_j + \frac{1}{2}\sum_{jk} \mathscr{H}_{jk} \quad . \tag{1}$$

The first term in Eq. (1) corresponds to the magnetic and quadrupolar energies of a single nucleus:

$$\mathscr{H}_j = -\gamma\hbar H I_{zj} + \frac{e^2 Q}{4I(2I-1)}\left(3I_{zj}^2 - I(I+1)\right)V_{zz}(j) \tag{2}$$

the z-axis of the coordinate system is directed along the applied field H. In the framework of the ABCM, the EFG (in units of the proton charge e) equals

$$V_{zz}(j) = -\sum_k (1-\gamma_\infty)\frac{Z_a}{\varepsilon} c_{jk} + \sum_p \left(1-\gamma(r_{jp})\right)\frac{Z_b}{\varepsilon} c_{b,jp} \ , \tag{3}$$

where $c_{jk} = \left(r(jk)^2 - 3z(jk)^2\right)/r(jk)^5$, $c_{b,jp} = (r_{jp}^2 - 3z_{jp}^2)/r_{jp}^5$, $\varepsilon = 16$ is the static dielectric constant [6], $\mathbf{r}(jk)$ and $\mathbf{r}_{jp}$ are vectors connecting j, k lattice sites, and j is the site with the bond charge p, respectively. Sternheimer antishielding factors $\gamma(r)$ in the general case depend on the distance r between the point charge and the nucleus. We use in this work two different values of the Sternheimer antishielding factor, which have been approved in [8] by calculations of the spin-lattice relaxation rates: $1 - \gamma_b = 30.86$ for the EFG due to the nearest bond charges, and $1 - \gamma_\infty = 100$ for the EFG due to all other atoms and charges.

The second term in Eq. (1) represents the secular part of the magnetic dipole-dipole interaction:

$$\mathscr{H}_{jk} = \frac{1}{2}\gamma^2\hbar^2 c_{jk}(3I_{zj}I_{zk} - \mathbf{I}_j\mathbf{I}_k) \quad . \tag{4}$$

An isolated ^{73}Ge atom has the equidistant Zeeman spectrum with a single resonance frequency independent of the direction of the applied magnetic field. Both the magnetic dipole-dipole interaction and the EFG induced by local lattice deformations change the Zeeman splittings, and the shape of the spectrum in a real crystal depends on the magnetic field direction.

The crystal lattice consists of two Bravais sublattices with sites defined by vectors $\mathbf{r}_{N\lambda} = a[n_1(1/2,\ 0,\ 1/2) + n_2(0,\ 1/2,\ 1/2) + n_3(1/2,\ 1/2,\ 0)] + \mathbf{R}_\lambda$, where $N = \{n_1n_2n_3\}$, $\mathbf{R}_1 = 0$, $\mathbf{R}_2 = (a/4)(1,\ 1,\ 1)$. The neighbors of a site $N\lambda$ are labeled below by the index i and have radius-vectors $\mathbf{r}_{N\lambda i} = \mathbf{r}_{N\lambda} + \mathbf{r}_i$ (i = 1–4 for the nearest bond charges, i = 5–8 for Ge atoms in the first coordination shell, i = 9–20 for the next nearest bond charges, and i = 21–32 for Ge atoms in the second coordination shell). In a perfect germanium crystal, the EFG at lattice sites is zero.

The isolated mass defect in the lattice site $N\lambda$ induces a totally symmetric local lattice deformation. Components of the displacement vector $\delta\mathbf{r}_i$ of the i-th neighbor, having a charge eq_i, are denoted below as δx_i, δy_i, δz_i. This mass defect induces a change of the EFG at the origin of the coordinate system, where we place a ^{73}Ge nucleus. Using an approximation, linear in $\delta\mathbf{r}_i$, we obtain

$$\delta V_{zz}(N\lambda) = -\sum_i \left(1 - \gamma(r_{N\lambda i})\right)\frac{3q_i}{\varepsilon r_{N\lambda i}^4}\left(V_3^1(N\lambda i)\,\delta x_i + V_3^{-1}(N\lambda i)\,\delta y_i + V_3^0(N\lambda i)\,\delta z_i\right) \quad . \tag{5}$$

Here $V_p^k(N\lambda i)$ are the spherical polynomials of an order p ($V_3^1 = (5z^2 - r^2)x/r^3$, $V_3^{-1} = (5z^2 - r^2)y/r^3$, $V_3^0 = (5z^2 - 3r^2)z/r^3$) proportional to the corresponding tesseral harmonics dependent on spherical angular coordinates of the vector $\mathbf{r}_{N\lambda i}$ [9]. At the large distance r from the mass defect a change of the crystal electric field potential due to a local lattice deformation can be presented as a series expansion in powers of $1/r$ in the following invariant form

$$\delta V(\mathbf{r}) = -\sum_i \frac{q_i}{\varepsilon}\left(\frac{15}{2r^4}\mathbf{r}\frac{\delta\mathbf{r}_i}{r}\left(\mathbf{r}\frac{\mathbf{r}_i}{r}\right)^2 + \frac{r_i^2}{r^5}(\mathbf{r}_i\delta\mathbf{r}_i) + \mathrm{O}\frac{1}{r^6}\right) \quad . \tag{6}$$

Let us denote radial displacements of Ge atoms in the first coordination shell of a single impurity isotope as $\sqrt{3}\delta_a$, radial displacements of the nearest bond charges as $\sqrt{3}\delta_b$, the displacement vector of the bond charge with coordinates $(a/8)(1,\ 3,\ 3)$ as $(\delta_{b1},\ \delta_{b2},\ \delta_{b2})$; displacements of other bond charges in this coordination shell can be obtained by the symmetry operations. It follows from results of calculations, reviewed in the appendix, that displacements of more distant atoms and bond charges do not exceed 1/10 of the nearest neighbor (nn) displacements. Calculated parameters of the local lattice deformation at several different temperatures are given in Table 1.

Table 1. Parameters of local deformations induced by impurity isotope centers in Ge crystals (in units of 10^{-6} nm per unit mass difference).

Deformation	Parameter	Value at temperature (K) 0	80	300	450
Single impurity atom	δ_b	−0.18	−0.13	−0.08	−0.05
	δ_a	−0.85	−0.61	−0.21	−0.11
	δ_{b2}	−0.020	−0.018	−0.004	0
	δ_{b1}	−0.047	−0.042	−0.010	0
First nn pair	δ_a^f	−1.18	−0.79	−0.29	−0.13
	δ_{a1}^f	−0.92	−0.68	−0.25	−0.11
	δ_{b1}^f	0.11	0.08	0.04	0.01
	δ_{b2}^f	−0.72	−0.59	−0.16	−0.08
Second nn pair	δ_a^s	−1.80	−1.36	−0.50	−0.22
	δ_{b1}^s	−0.21	−0.15	−0.08	−0.05
	δ_{b2}^s	−0.14	−0.09	−0.08	−0.05

Anisotropic properties of the cubic lattice reveal themselves by different responses on the external perturbations along tetragonal and trigonal symmetry axes. In the first case, when $\mathbf{H} \| [001]$, from the first term in the series Eq. (6), we obtain the EFG caused by the redistribution of the crystal charge density in the vicinity of the mass defect in the following form

$$\delta V_{zz}(N\lambda) = \mp 90(1-\gamma_\infty)\frac{a^2}{64}\frac{Z_b}{\varepsilon}\Delta V_5^{-2}(N\lambda)\frac{1}{r_{N\lambda}^6} \quad , \tag{7}$$

where $\Delta = 8\delta_a - \delta_b - 9\delta_{b1} - 6\delta_{b2}$. In the second case, when $\mathbf{H} \| [111]$, we use the linear transformation $x' = (x-y)/\sqrt{2}$, $y' = (x+y-2z)/\sqrt{6}$, $z' = (x+y+z)/\sqrt{3}$, and obtain

$$\delta V_{zz}(N\lambda) = \mp 10\sqrt{3}(1-\gamma_\infty)\frac{a^2}{64}\frac{Z_b}{\varepsilon}\Delta\left(5V_5^0(N\lambda) + \sqrt{2}V_5^{-3}(N\lambda)\right)\frac{1}{r_{N\lambda}^6} \quad , \tag{8}$$

the upper and lower signs in Eqs. (7) and (8) correspond to sites of the first and second sublattices, respectively. Due to the strong dependence of the induced EFG Eq. (7) and (8) on the distance $r_{N\lambda}$, the most essential changes of the equidistant Zeeman spectrum may be expected when the magnetic nucleus ^{73}Ge and the mass defect are close to one another. In the real samples, we have to consider the ^{73}Ge atom itself as an impurity center, and correlations between this atom and mass defects in its surroundings are to be taken into account. As can be seen in Table 1, where calculated parameters characterizing the local structure of impurity dimer isotope centers are presented, these correlations enhance relative atomic displacements in the first nearest neighbor pair up to 40%. This pair center (for example, two identical mass defects in the sites (0, 0, 0) and (a/4)(1, 1, 1), see Fig. 1a) has trigonal symmetry, its local structure can be characterized by four parameters:

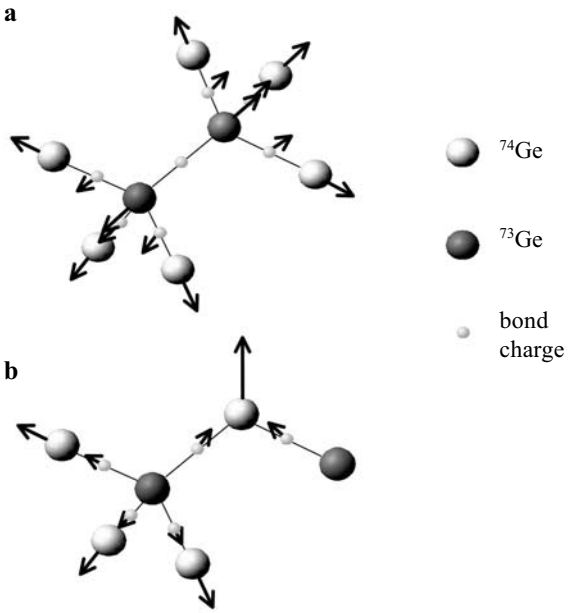

Fig. 1. First (**a**) and second (**b**) nearest neighbor impurity ^{73}Ge pairs in the ^{74}Ge crystal lattice.

$\sqrt{3}\delta_{\mathrm{a}}^{\mathrm{f}}$, displacements of the impurity atoms in opposite directions along the pair axis, $\sqrt{3}\delta_{\mathrm{al}}^{\mathrm{f}}$, radial displacements of the six nearest neighbor Ge atoms, displacement vectors of bond charges on the corresponding six bonds are determined by two parameters, in particular, $\delta\mathbf{r} = (\delta_{\mathrm{b}1}^{\mathrm{f}},\ \delta_{\mathrm{b}2}^{\mathrm{f}},\ \delta_{\mathrm{b}2}^{\mathrm{f}})$ for the bond charge at the site $(a/8)(1,\ -1,\ -1)$. Taking into account interactions of the nuclear quadrupole moment with the four nearest bond charges and four nearest atoms, we obtain

$$\delta V_{zz}(000,2) = D\left(8(1-\gamma_{\mathrm{b}})(20\delta_{\mathrm{a}}^{\mathrm{f}} + \delta_{\mathrm{b}1}^{\mathrm{f}} + 10\delta_{\mathrm{b}2}^{\mathrm{f}}) - (1-\gamma_{\infty})(29\delta_{\mathrm{a}}^{\mathrm{f}} - 9\delta_{\mathrm{a}1}^{\mathrm{f}})\right) \quad , \quad (9)$$

where $D = (16/3)^{5/2}(Z_{\mathrm{b}}/\varepsilon a^4)$. If the symmetry axis of the nearest neighbor pair is declined from the magnetic field direction [111] (there are three such pairs), the EFG equals $-\delta V_{zz}(000,2)/3$. From Eq. (9) and with the local deformation parameters given in Table 1, we obtain quadrupole shifts of the resonance frequencies in the nearest neighbor impurity ^{73}Ge pairs in perfect ^{74}Ge or ^{72}Ge crystals as much as 90 Hz at room temperature (this estimate increases by no more than 7% when the summation over the infinite lattice is accomplished). These shifts have the same order of magnitude and are even larger than contributions of the magnetic dipole-dipole interaction into the nuclear energies, namely these shifts determine the total spread of the NMR spectra in the magnetic field directed along the trigonal symmetry axis of a crystal.

The next nearest-neighbor impurity pair center (in particular, two identical mass defects in sites (0, 0, 0) and $(a/2)(1, 0, 1)$, see Fig. 1b) has rhombic symmetry.

In this case, we can neglect displacements of the impurity atoms; the displacement (0, δ^s_a, 0) of the Ge atom, which is the common nearest neighbor of both impurity atoms, is perpendicular to the pair axis, and displacements of the corresponding bond charges in sites (a/8)(1, 1, 1) and (a/8)(3, 1, 3) are denoted as (δ^s_{b2}, δ^s_{b1}, δ^s_{b2}) and ($-\delta^s_{b2}$, δ^s_{b1}, $-\delta^s_{b2}$). Calculated values of displacements are given in Table 1. Quadrupole shifts of the resonance frequencies in these twelve second nn pairs are nonzero when the magnetic field is directed along [001] or [111] axes, but their values are by an order of magnitude less than the shifts in the first nn-pairs in the field $\mathbf{H} \| [111]$. In particular, in the field $\mathbf{H} \| [001]$, the EFG at the site (000) caused by the impurity ^{73}Ge atom at the site (a/2)(1, 1, 0) (four equivalent positions in the lattice) or at the site (a/2)(1, 0, 1) (eight equivalent positions) can be written as follows

$$\delta V_{zz}(001,1) = -2\,\delta V_{zz}(100,1) = D\left(16(1-\gamma_b)(\delta^s_{b2} - \delta^s_{b1}) + 2(1-\gamma_\infty)\delta^s_a\right) , \quad (10)$$

and the corresponding shifts of the resonance line in second nn pairs do not exceed 7.8 Hz at room temperature. The EFG in pairs formed by different impurity isotopes were calculated assuming the linear dependence of the deformation parameters on the differences between the impurity isotope mass and the average mass of an atom in the crystal.

It is well known that point defects induce lattice strains [9]. In the framework of the elastic continuum approximation, displacements of atoms from the perfect lattice sites at large distances r from the mass defect δm can be presented as

$$\delta\mathbf{r} = -\frac{a^2}{4\pi}\frac{1+\sigma}{1-\sigma}\left(\frac{\delta a}{\delta m}\right)\delta m\frac{\mathbf{r}}{r^3} ,$$

where σ is the Poisson coefficient, and $\delta a/\delta m$ is the lattice constant change per unit isotope mass (see appendix). The EFG caused by strains due to a mass defect in the site $N\lambda$ equals

$$\delta V^s_{zz}(N\lambda) = \frac{3a^2}{4\pi}\left(\frac{\delta a}{\delta m}\right)\delta m\frac{1+\sigma}{1-\sigma}B(\mathbf{H}/H)\frac{V^0_2(N\lambda)}{r^3_{N\lambda}} , \quad (11)$$

where the coupling constant

$$B(\mathbf{H}/H) = \sum_i q_i\left(1-\gamma(r_i)\right)\frac{V^1_3(i)x_i + V^{-1}_3(i)y_i - 2V^0_3(i)z_i}{2\varepsilon r_i^4} \quad (12)$$

(the sum is over all atoms and bond charges at distances $r_i \ll r_{N\lambda}$) depends on the z-axis direction relative to the crystallographic axes. The calculated values of coupling constants, which correspond to the principal orientations of the magnetic

field, equal $e^2QB(\mathbf{H} \| [001]) = 12.7$ MHz, and $B(\mathbf{H} \| [111]) = -2B(\mathbf{H} \| [001])/3$ (it should be noted that trigonal strains induce relative displacements of the two Bravais sublattices in a Ge crystal, and the latter relation between the coupling constants actually is not valid beyond the elastic continuum approximation). It follows from a comparison of expressions Eqs. (7) and (8) with Eq. (11) that the long-range interactions between a nuclear quadrupole moment and lattice strains already prevail over the short-range interaction with local electric multipoles at the defect sites at distances between the ^{73}Ge atom and the impurity isotope larger than 2–3 lattice constants. However, the relation between the coupling constants presented above may cause a more pronounced isotopic-disorder effect in the magnetic field $\mathbf{H} \| [001]$ than in the field $\mathbf{H} \| [111]$, but this is not the case experimentally (see Sect. 3).

Due to a chaotic distribution of atoms with different masses over the lattice sites, we can consider quadrupole moments of ^{73}Ge in the random crystal fields with the EFG represented by a sum of expressions Eqs. (7)–(11) multiplied by the occupation numbers (which are random variables equal to 0 or 1) of the lattice sites. The distribution functions for the resonance frequencies corresponding to transitions $\pm m_I \leftrightarrow \pm(m_I + 1)$ ($m_I = 1/2,\ 3/2,\ 5/2,\ 7/2$) can be characterized by their moments. The second moment equals (we neglect correlations between mass defects)

$$M_2(m_I) = \langle(\nu_{m_I} - \nu_0)^2\rangle = (\langle m\rangle g_2)^2 \sum_{N\lambda} \delta\nu_{m_I}^2(N\lambda) \quad , \tag{13}$$

where $\nu_0 = (\gamma/2\pi)H$, $\langle m\rangle$ is the average atomic mass in the crystal,

$$g_n = \frac{\langle \Delta m^n\rangle^{1/n}}{\langle m\rangle} \quad , \tag{14}$$

and

$$\delta\nu_{m_I}(N\lambda) = \frac{3e^2Q(2m_I + 1)}{8\pi\hbar I(2I - 1)} \delta V_{zz}(N\lambda) \quad . \tag{15}$$

The shape of the distribution can be characterized (qualitatively) by the ratio of the fourth moment to the squared second moment

$$\kappa_{\mathrm{Q}} = \frac{M_4}{3M_2^2} = 1 + \left(\frac{g_4}{g_2}\right)^4 \frac{\sum_{N\lambda} \delta\nu_{m_I}^4(N\lambda)}{3\left(\sum_{N\lambda} \delta\nu_{m_I}^2(N\lambda)\right)^2} \quad . \tag{16}$$

This ratio is independent of m_I (we would like to emphasize here that the transition $-1/2 \leftrightarrow 1/2$ is not influenced by the random crystal field); if $\kappa_{\mathrm{Q}} = 1$, the distribution is of the Gauss type, and if $\kappa_{\mathrm{Q}} \gg 1$, it is of the Lorentz type. The Gaussian shape of the distribution function can be derived if additivity of ran-

dom lattice deformations is supposed, and the impurity concentration is large enough [9] (it should be noted that the second term in the right-hand side of Eq. (16) diminishes with the increasing isotopic disorder).

As the simplest approximation for the NMR line shape, we can use the sum of weighted Gaussians corresponding to individual magnetic dipole transitions $m_I \leftrightarrow m_{I\pm1}$. In the case of convoluted Gaussians corresponding to quadrupole and magnetic mechanisms of the line broadening, we obtain

$$f(\nu) = \left(\int f(\nu)\,\mathrm{d}\nu\right) \frac{\sum_{m=-7/2}^{m=9/2} \frac{|\langle m|I_x|m-1\rangle|^2}{\left((2m-1)^2 b^2/4 + d^2\right)^{1/2}} \exp\left(-\frac{\nu^2}{(2m-1)^2 b^2/4 + d^2}\right)}{\pi^{1/2} \sum_{m=-7/2}^{m=9/2} |\langle m|I_x|m-1\rangle|^2}, \quad (17)$$

where $b^2 = 2M_2(1/2)$, and the parameter d characterizes the magnetic linewidth. Long tails of the NMR signal are to be expected: in particular, for the Gaussian line shape, the ratio of the full width at 1/20 of line height (which may be considered as a plateau width in the measured spectra) to the full width at half height equals 2.078, for function Eq. (17) this ratio increases up to 3.445. The nearest neighbor pairs do not contribute to the linewidth in the field $\mathbf{H} \parallel [001]$, thus the minimum and maximum values of linewidths may be expected for $\mathbf{H} \parallel [001]$ and $\mathbf{H} \parallel [111]$, respectively. The calculated values of κ_Q ratios and quadrupole linewidths in the real Ge samples are discussed below. In numerical simulations, we neglected interactions of magnetic nuclei with lattice strains at large distances from the impurity isotopes because it is difficult to estimate errors caused by the elastic continuum approximation.

3 Experimental Details and Results

NMR spectra of ^{73}Ge have been measured for three single crystals ($6\times6\times6$ mm^3) of the purest germanium (carrier concentration $n_{carr} \sim 10^{12}$ cm^{-3} at 290 K) with different isotopic compositions. One of the crystals "Ge-*n*" was synthesized from the material with natural isotope abundance [10]. Much lower level of the isotopic disorder was reached in two other crystals (see Table 2). The isotopic con-

Table 2. Isotopic composition of Ge samples.

Sample	$\langle m \rangle$	Isotope content (%)					$100g_2$	$100g_4$
		^{70}Ge	^{72}Ge	^{73}Ge	^{74}Ge	^{76}Ge		
Ge-0.1	70.03	96.3	2.1	0.1	1.2	0.3	0.880	2.30
Ge-3	73.91	0.1	0.9	3.8	92.6	2.6	0.596	1.30
Ge-*n*	72.61	20.84	27.54	7.73	36.28	7.61	2.424	2.95
Isotope atomic weight		69.924	71.922	72.923	73.921	75.921		

tent of the sample "Ge-0.1" with very low concentration of magnetic nuclei ^{73}Ge presented the possibility to suppress the magnetic dipole mechanism of the line broadening. The samples were prepared following the procedure described elsewhere [11]. The degree of the isotopic disorder in different samples can be characterized by the parameters g_n (see Eq. (14)) presented in Table 2. The electron microscopy studies confirm the presence of extremely low total density of dislocations ($n_{\mathrm{disl}} < 10^3$ cm^{-2}). This permits us to exclude from the following consideration a possible influence of traditional defects [1–3] as a source of quadrupole broadening of the NMR line measured for all three single crystals.

The NMR measurements were performed at room temperature with the phase coherent pulse NMR spectrometers operating at frequencies $\nu = 3.6$ and 17.44 MHz (the ^{73}Ge NMR spectra taken at the frequency of 17.44 MHz are shown in Figs. 2 and 3 for $\mathbf{H} \parallel [111]$ and $\mathbf{H} \parallel [001]$, respectively). Inhomogeneity of the static magnetic field was minimized by standard shimming procedure to 0.2 ppm within the sample. Duration of the exciting $\pi/2$ pulse did not exceed 15 μs. Its spectral width was enough to excite uniformly the whole spectrum of ^{73}Ge. In experiments with single exciting pulse, the ^{73}Ge free induction decay (FID) signal was measured. After Fourier transformation of the FID a peak of the NMR

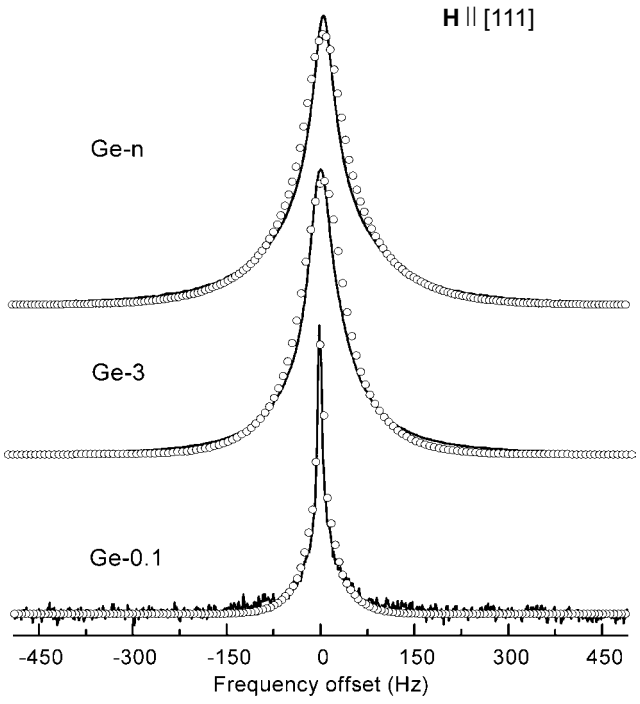

Fig. 2. NMR spectra of Ge samples taken at room temperature in the magnetic field 12 T along the crystal trigonal symmetry axis. Solid lines present experimental data, open circles present the function Eq. (18).

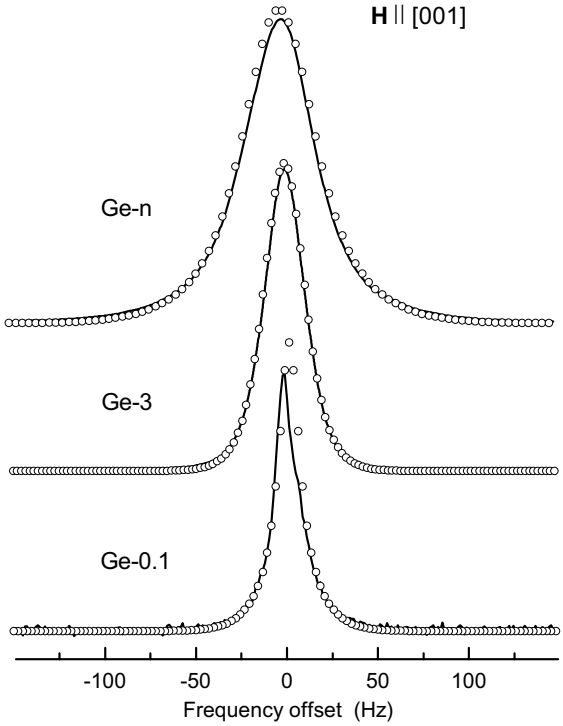

Fig. 3. NMR spectra of Ge samples taken at room temperature in the magnetic field 12 T along the crystal tetragonal symmetry axis. Solid lines present experimental data, open circles present the function Eq. (18).

line was found to be shifted at $\delta\nu/\nu = -108(2)$ ppm with respect to the peak of the ^{73}Ge line in a water solution of $GeCl_4$, used as a reference (V. Privalov and V. Tarasov, pers. commun.).

We studied with care the influence of the magnetic interactions linear in nuclear spin operators on the spectra (the corresponding effects depend on the inhomogeneity of the magnetic field within a sample, the demagnetizing field, and the distribution of chemical shifts). As the result of measurements at different frequencies, we found that the width of the central peak ($-1/2 \leftrightarrow 1/2$ transitions) was independent of ν for Ge-*n* and Ge-3 samples. Independently, the ^{73}Ge spectra in these crystals were obtained at the frequency $\nu = 13.55$ MHz as the Fourier transformation of the spin-echo amplitude envelope $A(2t_i)$ in the following sequence:

$$\{(\pi/2)_x - t_i - \pi_x - t_i - \text{echo} - 5T_1 - (\pi/2)_{-x} - t_i - \pi_x - t_i - \text{echo} - 5T_1\}_n$$

with t as a variable parameter. Here T_1 is the nuclear spin-lattice relaxation time of ^{73}Ge. The doubled step of the time interval between a pair of exciting pulses $\Delta t = t_{i+1} - t_i$ is taken to be equal to $\Delta t = 400$ μs, and it plays the role of the

dwell time for the array $\{A(2t_i)\}$. The maximal duration of $t_n = 120$ μs determined a resolution $\Delta\nu = 1/t_n = 8$ Hz of the spectra obtained. In these echo experiments the inhomogeneity of the constant magnetic field within the sample was less than 300 Hz. The relative inhomogeneity of exciting radio-frequency (rf) field within a sample did not exceed 10% and was determined by properly chosen diameter of the rf coil. As is well known, the magnetic interactions linear in nuclear spin operators do not contribute to the $A(2t)$ envelope in these spin-echo experiments if the symmetry of the EFG tensor is close to axial [2, 12]. Within accuracy of a given spectral resolution these "echo" spectra measured at $\mathbf{H} \parallel [001]$ presented the same width of the central peak ($-1/2 \leftrightarrow 1/2$) as the "FID" spectra shown in Fig. 3, and a similar increase of the wing intensities was found in "echo" spectra measured at $\mathbf{H} \parallel [111]$. From these additional experiments, we have found that the main peculiarities of the line shapes are due to the combined effect of the quadrupole and magnetic interactions bilinear in nuclear spin operators.

The measured spectra were analyzed with the assumed line shape (see Eq. (17))

$$f(\nu) = \frac{M_0}{165\sqrt{\pi}}\left[\frac{25}{d}\exp\left(-\frac{\nu^2}{d^2}\right) + \frac{48}{\sqrt{d^2+b^2}}\exp\left(-\frac{\nu^2}{d^2+b^2}\right) + \frac{42}{\sqrt{d^2+4b^2}}\exp\left(-\frac{\nu^2}{d^2+4b^2}\right) + \frac{32}{\sqrt{d^2+9b^2}}\exp\left(-\frac{\nu^2}{d^2+9b^2}\right) + \frac{18}{\sqrt{d^2+16b^2}}\exp\left(-\frac{\nu^2}{d^2+16b^2}\right)\right], \tag{18}$$

where M_0 is the NMR line zero moment. The quadrupole and magnetic contributions are characterized by the full widths at the half height of the resonance line $\Delta\nu_Q = 2(\ln 2)^{1/2}b$, $\Delta\nu_M = 2(\ln 2)^{1/2}d$ of the $\pm 1/2 \leftrightarrow \pm 3/2$ (in the absence of the magnetic contribution) and $-1/2 \leftrightarrow +1/2$ transitions, respectively. The obtained parameters of the line shapes are presented in Table 3, and the calculated spectral envelopes are compared with the experimental data in Figs. 2 and 3.

Table 3. Parameters of fit with expression Eq. (18) of the measured NMR line shapes at room temperature (in Hz). Magnetic ($\Delta\nu_M$) and quadrupole ($\Delta\nu_Q$, $\pm 1/2 \leftrightarrow \pm 3/2$ transitions) widths calculated in Gaussian approximation following Eqs. (19) and (13) are given in brackets. Columns κ_Q and κ_M contain the calculated ratios of the fourth moment to the tripled square of the second moment for the distribution functions of the quadrupole and magnetic shifts of the resonance line, respectively.

Sample	$\mathbf{H} \parallel [001]$				$\mathbf{H} \parallel [111]$			
	$\Delta\nu_Q$	κ_Q	$\Delta\nu_M$	κ_M	$\Delta\nu_Q$	κ_Q	$\Delta\nu_M$	κ_M
Ge-*n*	27.8 (25.4)	1.03	32.5 (25.1)	1.06	93.2 (113.8)	1.12	50.0 (71.0)	3.42
Ge-3	11.4 (6.1)	1.31	20.2 (17.6)	1.28	66.6 (28.5)	2.24	48.0 (49.8)	6.01
Ge-0.1	13.0 (9.1)	1.63	8.5 (2.9)	17.8	34.1 (39.8)	3.56	9.6 (8.1)	194.9

Temperature variations of the fitting parameters for the NMR lines in the Ge-3 sample measured in spin-echo experiments at the frequency of 13.55 MHz:

$$\mathbf{H} \| [001]: \Delta\nu_Q = 30 \text{ Hz (80 K)}, 27 \text{ Hz (300 K)}, 24 \text{ Hz (450 K)}, \quad \Delta\nu_M = 16 \text{ Hz},$$

$$\mathbf{H} \| [111]: \Delta\nu_Q = 196 \text{ Hz (80 K)}, 158 \text{ Hz (300 K)}, 150 \text{ Hz (450 K)}, \quad \Delta\nu_M = 56 \text{ Hz},$$

may be considered as rough estimates only due to rather low signal-to-noise ratio in the corresponding experimental spectra. Calculated relative changes of $\Delta\nu_Q$ with the temperature are the following:

$$\mathbf{H} \| [001]: 1 \text{ (0 K)} : 0.72 \text{ (80 K)} : 0.294 \text{ (300 K)} : 0.145 \text{ (450 K)},$$

$$\mathbf{H} \| [111]: 1 \text{ (0 K)} : 0.72 \text{ (80 K)} : 0.325 \text{ (300 K)} : 0.160 \text{ (450 K)}.$$

Comparison with the experimental data shows that theory predicts much stronger effect (temperature narrowing) than the observed diminishing of the quadrupole contributions to the line broadening.

4 Discussion

A comparison of the calculated and measured line shapes given in Figs. 2 and 3 shows that there are specific peculiarities of the NMR signals in crystals with the isotopic disorder which cannot be described by the assumed superposition of the Gaussians. These peculiarities (the "logarithmic type" line shape) are very expressive in the spectra taken in the magnetic field parallel to the trigonal symmetry axis of Ge crystal (Fig. 2).

The quadrupole contributions $\Delta\nu_Q$ to the line widths were calculated in accordance with Eq. (13), supposing the Gaussian line shape, and are given in brackets in Table 3. In this case $\Delta\nu_Q$ should be a linear function of the parameter g_2 which determines the isotopic disorder in the sample. In all cases considered, calculated and experimental values of $\Delta\nu_Q$ agree satisfactorily (see Table 3), except the spectra of the Ge-3 sample. The expected ratios of the quadrupole widths in the samples Ge-0.1–Ge-3–Ge-n (1 : 0.68 : 2.75) are consistent qualitatively with the experimental data for $\mathbf{H} \| [001]$, 1 : 0.87 : 2.14, but there is a remarkable contradiction with the data for $\mathbf{H} \| [111]$, 1 : 1.95 : 2.73. The Ge-3 sample has the minimum g_2 value, about 1.5 times less than that in the Ge-0.1 sample (see Table 2), but the width of the plateau in the NMR signal in this sample in the case of $\mathbf{H} \| [111]$ is more than 2.5 times larger than that in the corresponding NMR line in the Ge-0.1 sample.

Magnetic components of linewidths can be estimated considering the corresponding contributions to moments of the NMR line [2, 14]. Taking into account the secular terms Eq. (4) in magnetic dipole-dipole interactions, one ob-

tains the following expressions for the second and fourth moments of the resonance line [13]:

$$M_{m,2} = \frac{3\gamma^4\hbar^2 c}{4(2\pi)^2} I(I+1)\sum_{\mathrm{k}} c_{0k}^2 \quad , \tag{19}$$

$$M_{m,4} = 3M_{m,2}^2 + \left(\frac{3\gamma^4\hbar^2 c}{4(2\pi)^2} I(I+1)\right)^2 \times\left[\frac{1}{5c}\left(7 - \frac{3}{2I(I+1)}\right)\sum_k c_{0k}^4 - \frac{1}{3}\sum_{j\neq k\neq 0} c_{jk}^2 (c_{0k} - c_{0j})^2\right] . \tag{20}$$

Carrying out lattice summations, we obtained the ratios $\kappa_{\mathrm{M}} = M_{m,4}/3M_{m,2}^2$ as explicit functions of the concentration c of magnetic nuclei: $\kappa_{\mathrm{M}}(\mathbf{H} \| [001]) = 0.8326 + 0.01694/c$; $\kappa_{\mathrm{M}}(\mathbf{H} \| [111]) = 0.8203 + 0.1941/c$. Numerical values of κ_{M} in our samples are given in Table 3 (it should be noted that the contributions due to the pseudo-dipolar interactions between the ^{73}Ge atoms may be significant as well). In the Ge-0.1 sample, for both orientations of the magnetic field, and in the Ge-3 sample for $\mathbf{H} \| [111]$ ratios κ_{M} exceed 1 considerably. In these cases the Lorentzian line shape might be more appropriate to describe the magnetic broadening. The full width at the half height of the Lorentzian can be estimated as $\Delta\nu_{\mathrm{ML}} = \pi\Delta\nu_{\mathrm{M}}/(72\kappa_{\mathrm{M}}\ln 2)^{1/2}$, where $\Delta\nu_{\mathrm{M}} = 2(2M_{m,2}\ln 2)^{1/2}$ [2]. However, the corresponding results do not agree with the experimental data: values of $\Delta\nu_{\mathrm{ML}}$ are too low and only slightly dependent on the magnetic field direction; in particular, for Ge-0.1 sample we obtain 0.31–0.26 Hz, and for the Ge-3 sample 6.92–9.03 Hz in magnetic fields along [001] and [111] directions, respectively.

If we neglect the effect of magnetic field imhomogeneity on the line shape, we can consider the magnetic contribution to the linewidth ($\Delta\nu_{\mathrm{M}}$) as a function of the concentration c of magnetic nuclei. An examination of $\Delta\nu_{\mathrm{M}}$ values obtained by the fitting procedure (see Table 3) gives evidence that the approximation $\Delta\nu_{\mathrm{M}}(c) \sim c^{1/2}$, which is consistent with the assumed Gaussian line shape, describes variations of $\Delta\nu_{\mathrm{M}}$ through the set of Ge-0.1, Ge-3, Ge-n samples with remarkable errors (ratios of the square roots $c^{1/2}$ equal 1 : 6.16 : 8.79, and the relative changes of the magnetic linewidths are 2.58 : 6.16 : 9.88 for $\mathbf{H} \| [001]$ and 1.23 : 6.16 : 6.42 for $\mathbf{H} \| [111]$). The calculated linewidths $\Delta\nu_{\mathrm{M}}$, presented in Table 3, agree only qualitatively with the data obtained by the fitting procedure, a large difference for the Ge-0.1 sample in the field $\mathbf{H} \| [001]$ might be expected because in this case the dipolar contribution is comparable with the linewidth ($\approx$4 Hz) caused by the external magnetic field distribution.

The dramatic change of the NMR line shape with the orientation of the magnetic field takes its origin in the structure and symmetry of the nearest-neighbor and next-nearest-neighbor pair impurity centers containing one or two magnetic nuclei. Examples of NMR spectra of the isolated impurity isotope pair are given in Figs. 4 and 5 for $\mathbf{H} \| [001]$ and $\mathbf{H} \| [111]$ respectively and represent results of

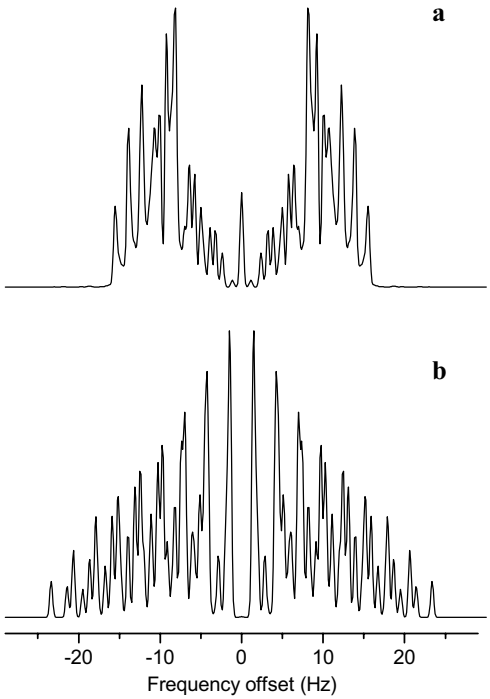

Fig. 4. Calculated envelopes of the NMR spectra of the isolated impurity isotope pair in the ^{74}Ge crystal in the magnetic field $\mathbf{H} \parallel [001]$: two ^{73}Ge atoms at the sites (0, 0, 0) and (a/2, a/2, 0) in the perfect (**a**) and locally deformed lattice (**b**).

the exact solution for Hamiltonian $\mathscr{H}_1 + \mathscr{H}_2 + \mathscr{H}_{12}$. Parameters of the local deformations correspond to room temperature and intrinsic widths of individual transitions of 0.7 Hz (Fig. 4) and 1.4 Hz (Fig. 5) have been used in final simulations. A comparison of Fig. 4a and b with Fig. 5b and c demonstrates obviously the different character of quadrupole effects, induced by local deformations of the lattice, on the magnetic nucleus subsystem under the tetragonal $\mathbf{H} \parallel [001]$ and trigonal $\mathbf{H} \parallel [111]$ perturbations. In the first case, the quadrupole interaction induced by local deformations assembles the spectrum close to the central line, and only slightly increases its total width (see Fig. 4a and b). Thus, in this case, a utilization of the Gaussian line shapes is even more appropriate (see Fig. 3) than in the case of a system containing a large concentration of magnetic impurities coupled through pure magnetic dipole interactions. In the second case, we observe an opposite effect (see Fig. 5b and c), quadrupole splittings devastate the central part of the spectrum, and increase essentially the pair spectrum width, forming a rather wide plateau in the spectra measured (see Fig. 2).

However, the plateau may appear not only due to the simultaneous action of magnetic dipole-dipole and electric quadrupole interactions. In crystals with a low concentration of magnetic nuclei, the plateau is formed by spectra of the nearest-

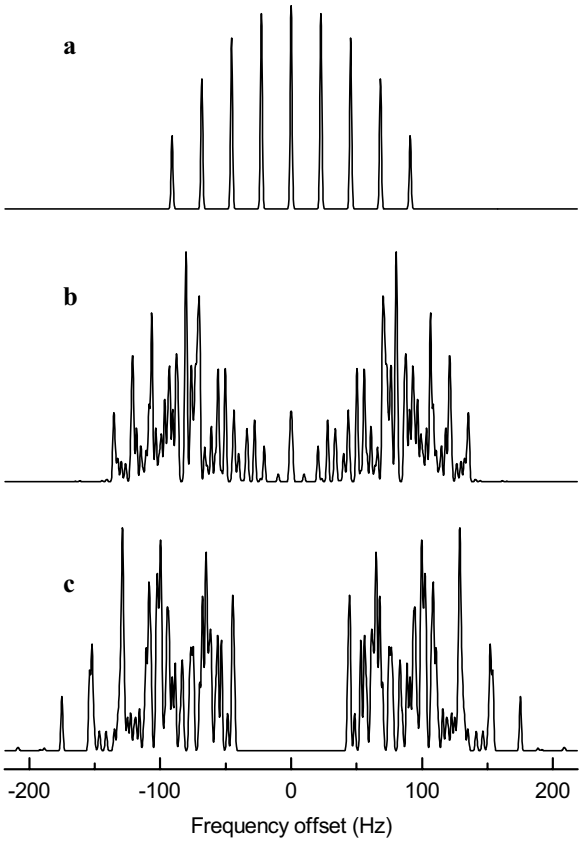

Fig. 5. Calculated envelopes of the NMR spectra of the isolated impurity isotope pair in the ^{74}Ge crystal in the magnetic field parallel to the pair axis: the nearest neighbor ^{73}Ge and ^{72}Ge atoms (**a**); the nearest neighbor ^{73}Ge atoms in the perfect (**b**) and locally deformed lattice (**c**).

neighbor impurity pairs that contain magnetic and nonmagnetic nuclei. The total width of the spectrum of these pairs is comparable with the splittings of the central line in spectra of magnetic pairs (see Fig. 5a), while the distribution of the separate line intensities approves again the Gauss type approximation for the line shapes of individual transitions. From arguments presented above, it follows that the case of intermediate concentrations of magnetic nuclei and relatively low concentrations of nonmagnetic isotopes, as in the Ge-3 sample, constitutes the most complex problem and demands a more thorough theoretical analysis.

5 Conclusion

NMR spectra of ^{73}Ge in three Ge samples with different isotopic composition have been measured at different frequencies and temperatures in magnetic fields along

the tetragonal and trigonal symmetry axes of the crystal lattice. We have unambiguously shown that the isotopic disorder causes some specific features of the first-order quadrupole broadening effects in the NMR spectra of nuclei with nonzero quadrupole moment. In particular, it was found for Ge crystals that local deformations, arising due to the isotope mass difference, led to the most intensive broadening effect for the magnetic field aligned along the trigonal symmetry axes, and as a consequence of quantum nature of the local deformations, the distribution width of the induced EFG was found to decrease with increasing temperature.

Experimental data obtained in this work have been analyzed with the results of calculations of the crystal lattice deformations in the vicinity of the isolated single and pair mass defects. Relations between the NMR spectral characteristics and the macroscopic (moments of the mass distribution) and microscopic (displacements of atoms induced by the impurity isotopes) parameters of the isotopic disorder have been derived. The constraints for analysis of the line shape developed under Gaussian approximation for the distribution function of quadrupolar and magnetic shifts have been considered. Though the induced lattice deformations are very small (atomic displacements are comparable with the nuclear dimensions), their influence on the NMR line shape is well pronounced, and we finish with the conclusion that NMR can be considered as a powerful control method in the isotopic engineering.

Appendix

Local Lattice Deformations Due to the Impurity Isotopes in Ge

The density functional approach [14], the quantum path-integral Monte Carlo method and the quasiharmonic approximation [15] were used in some earlier theoretical studies of Ge lattice constant dependence on the isotope composition. The calculated changes of the average unit cell dimensions are in quantitative agreement with the measured change of the lattice constant per unit isotope mass which equals $-6.29 \cdot 10^{-6}$ nm at 78 K and diminishes (in modulus) down to $-2.66 \cdot 10^{-6}$ nm at 300 K [16]. These data were corrected recently in [17], where an essentially weaker temperature dependence of the difference between lattice constants of crystals with different isotopic content was obtained.

In this work, parameters of the lattice deformations induced by single and pair impurity isotope centers in the Ge crystal have been obtained using a theoretical approach derived in [18–20]. Let us expand the potential energy Φ of a lattice containing isotope (mass) defects in a series in the static ($\mathbf{u}$) and dynamic ($\boldsymbol{\xi}$) displacements of atoms from their equilibrium positions in a regular lattice (a matrix form for contractions over the atom labels and coordinates is used):

$$\Phi = \Phi_0 + (1/2!)\mathbf{\Phi}^{(2)}(\mathbf{u} + \boldsymbol{\xi})^2 + (1/3!)\mathbf{\Phi}^{(3)}(\mathbf{u} + \boldsymbol{\xi})^3 + \ldots \qquad (1A)$$

Conditions for an equilibrium of a lattice $\partial\langle\Phi\rangle/\partial\mathbf{u} = 0$ provide a system of equations for the static displacements $\mathbf{\Phi}^{(2)}\mathbf{u} + (1/2!)\mathbf{\Phi}^{(3)}\langle\boldsymbol{\xi}\boldsymbol{\xi}\rangle + \ldots = 0$, where the an-

gular brackets denote averaging over the canonical ensemble of a harmonic lattice. Using a similar system of equations for the perfect lattice with the same matrices of the second ($\mathbf{\Phi}^{(2)}$) and third ($\mathbf{\Phi}^{(3)}$) order force constants, we can put down displacements of atoms induced by mass defects as follows:

$$\delta\mathbf{u} = (1/2)\mathbf{G}(\omega = 0)\mathbf{\Phi}^{(3)}(\langle\boldsymbol{\xi}\boldsymbol{\xi}\rangle - \langle\boldsymbol{\xi}\boldsymbol{\xi}\rangle_0) \ , \tag{2A}$$

where $\langle ... \rangle_0$ denotes the canonical averaging for the regular lattice, and the Green function of the defect lattice has been introduced:

$$G(\omega) = \left((\mathbf{m} + \delta\mathbf{m})\omega^2 - \mathbf{\Phi}^{(2)}\right)^{-1}. \tag{3A}$$

Here $\mathbf{m}$ is the diagonal (in the site representation) matrix of atom masses in the regular lattice, and $\delta\mathbf{m}$ represents mass changes due to the presence of impurity isotopes. The Green function matrix of the perturbed crystal can be expressed through the Green function $\mathbf{G}_0$ of the perfect crystal:

$$\mathbf{G} = \mathbf{G}_0 - \mathbf{G}_0(\mathbf{1} + \delta\mathbf{m}\omega^2\mathbf{G}_0)^{-1}\delta\mathbf{m}\omega^2\mathbf{G}_0 \ . \tag{4A}$$

Let us present components of the displacement vector (see Eq. (2A)) of an atom or a bond charge in the L-th unit cell and belonging to the k Bravais sublattice in the explicit form:

$$\delta u_\alpha\begin{pmatrix} L \\ k \end{pmatrix} = \frac{1}{2}\sum_{L'k'} \sum_{L''k'' \neq L'k'} \sum_{L'''k''' \neq L'k', L''k''} G_{\alpha\beta}\begin{pmatrix} L\,L' \\ k\;k' \end{pmatrix}\Phi^{(3)}_{\beta\gamma\zeta}\begin{pmatrix} L'\,L''\,L''' \\ k'\;k''\;k''' \end{pmatrix}\phi_{\gamma\zeta}\begin{pmatrix} L''\,L''' \\ k''\;k''' \end{pmatrix} \ , \tag{5A}$$

here repeated Greek indices are summed over, differences of the correlation functions for the perturbed and perfect lattices $\boldsymbol{\phi} = \langle\boldsymbol{\xi}\boldsymbol{\xi}\rangle - \langle\boldsymbol{\xi}\boldsymbol{\xi}\rangle_0$ can be calculated with the formula

$$\boldsymbol{\phi} = -(\hbar/2\pi)\int \left(2n(\omega) + 1\right)\mathrm{Im}\left(\mathbf{G}_0(1 + \delta\mathbf{m}\omega^2\mathbf{G}_0)^{-1}\,\delta\mathbf{m}\mathbf{G}_0\right)\omega\,\mathrm{d}\omega^2 \tag{6A}$$

($n(\omega)$ is the phonon occupation number). Infinite sums over the lattice sites in Eq. (5A) can be truncated when taking into account the rapid decrease of the differences $\boldsymbol{\phi}$ with the increase of the distance from the perturbed lattice site and neglecting all anharmonic force constants except those that correspond to the nearest neighbor atoms and bond charges. The third-order force constants $\Phi^{(3)}$ were obtained from the second-order force constants, the latter were assumed to depend on the bond lengths r and the bond directions as follows (similar dependences were used in [6]): $\Phi^{(2)}_{\mathrm{aa}}(r) = (r/r_{0,\mathrm{a}})^{m_\mathrm{a}}\Phi^{(2)}_{\mathrm{aa}}(r_{0,\mathrm{a}})$ for the pair non-Coulomb interaction between the nearest neighbor atoms, $\Phi^{(2)}_{\mathrm{ac}}(r) = (r/r_{0,\mathrm{ac}})^{m_\mathrm{ac}}\Phi^{(2)}_{\mathrm{ac}}(r_{0,\mathrm{ac}})$ for the non-Coulomb interaction between an atom and a bond charge, and for the coupling constant of the Keating three-body interac-

tion (bond charge-atom-bond charge) $V(r,\theta) = (r/r_{0,c})^{m_c}(\cos\theta/\cos\theta_0)^{l_c}V(r_{0,c},\theta_0)$. Here $r_{0,a} = a\sqrt{3}/4$, $r_{0,ac} = a\sqrt{3}/8$ are the bond lengths, $r_{0,c} = a\sqrt{2}/4$ is the distance between the nearest neighbor bond charges on the bonds shared by the angle θ_0 in the perfect lattice ($\cos\theta_0 = -1$). We used numerical values of exponents $m_c = -1.18$, $l_c = -2.54$ determined in [6]. Two other parameters of the model $m_a = -10.3$ (-12.73), $m_{ac} = -5.3$ (12.27) were determined from fitting of the calculated changes per unit isotope mass of the Ge lattice constant at 78 and 300 K to the values measured in [16]. Differences between our values of the exponents m_a, m_{ac} and those obtained in [6] (which are given above in brackets) are due to the neglect of the bond charge dependence on the bond length in our model.

Details of calculations and explicit shapes of Green function spectral densities in the monoisotopic Ge lattice were presented in [7]. The differences between the atom-atom, atom-bond charge, bond charge-bond charge correlation functions in the lattice with the single or pair mass defects (see Fig. 1) and in the perfect lattice were obtained by numerical integration and were checked by direct calculations of derivatives of correlation functions with respect to the mass of the impurity isotopes. Calculated parameters of the structure of the impurity centers are presented in Table 1. It should be noted that, in the framework of our model, we obtained the relative change of the Ge lattice constant per unit isotope mass of $-3.9 \cdot 10^{-6}$ at 300 K (that coincides with the value measured in [17]) and $-9.8 \cdot 10^{-6}$ at 78 K as compared with the approximately $-7 \cdot 10^{-6}$ value measured at this temperature in [17], thus results of our calculations in Table 1 for 0 and 80 K may be overestimated up to 40%.

Acknowledgements

The research was supported by Grants of CRDF (RP1-218) and INTAS (96-0546).

References

1. Cohen M.H., Reif F.: Solid State Physics (Seitz F., Turnbull D., eds.), vol. 5, p. 321. New York: Academic Press 1957.
2. Abragam A.: The Principles of Nuclear Magnetism. Oxford: Clarendon Press 1961.
3. Omini M., Sparavigna A.: Physica B **233**, 230 (1997)
4. Ozhogin V.I., Inyushkin A.V., Taldenkov A.N., Tikhomirov A.V., Popov G.E., Haller E., Itoh K.: Sov. Phys. JETP Lett. **63**, 490 (1996)
5. Weber W.: Phys. Rev. B **15**, 4789 (1977)
6. Eryigit R., Herman I.P.: Phys. Rev. B **53**, 7775 (1996)
7. Malkin B.Z., Saikin S.K., Ozhogin V.I.: Appl. Magn. Reson. **14**, 513 (1998)
8. Aminov L.K., Malkin B.Z., Teplov M.A.: Handbook on the Physics and Chemistry of the Rare-Earths (Gschneidner K.A., LeRoy Eyring, eds.), vol. 22, pp. 295–506. Amsterdam: North-Holland 1996.
9. Ivanov M.A., Mitrofanov V.Ya., Falkovskaya L.D., Fishman A.Ya.: J. Magn. Magn. Met. **36**, 26 (1983)
10. Timofeev Yu.A., Vinogradov B.V., Stishov S.M.: Sov. Phys. JETP Lett. **69**, 211 (1999).
11. Itoh K.: Doctoral Thesis, University of California at Berkeley, Berkeley, CA, USA 1994.

12. Boden N., Levine Y.K.: J. Magn. Reson. **30**, 327 (1978)
13. Al'tshuler S.A., Kozirev B.M.: Electron Paramagnetic Resonance. Moscow: Nauka 1972.
14. Pavone P., Baroni S.: Solid State Commun. **90**, 295 (1994)
15. Noya J.C., Herrero C.P., Ramirez R.: Phys. Rev. B **56**, 237 (1997)
16. Buschert R.C., Merlini A.E., Pace S., Rodriguez S., Grimsditch M.H.: Phys. Rev. B **38**, 5219 (1988)
17. Kazimirov A., Zegenhagen J, Cardona M.: Science **282**, 930 (1998)
18. Timmesfeld K.H., Elliott R.J.: Phys. Status Solidi **42**, 859 (1970)
19. Agladze N.I., Popova M.N., Koreiba M.A., Malkin B.Z., Pekurovskii V.R.: JETP **77**, 1021 (1993)
20. Malkin B.Z., Saikin S.K.: Tenth Feofilov Symposium on Spectroscopy of Crystals Activated by Rare-Earth and Transitional-Metal Ions (Ryskin A.I., Masterov V.F., eds.), Proc. SPIE **2706**, 193 (1996)

Authors' address: Prof. Dr. Boris Z. Malkin, Kazan State University, Kremlevskaya str. 18, Kazan 420008, Russian Federation